Kungl Tekniska Högskolan

Department of Numerical Analysis and Computer Science

TRITA-NA-0325 • ISSN 0348-2952 • ISRN KTH/NA/R--03/25--SE

# Stabilized Local Non-reflecting Boundary Conditions for High Order Methods

**Daniel Appelö and Gunilla Kreiss**

**Numerical Analysis**

Daniel Appelö and Gunilla Kreiss
*Stabilized Local Non-reflecting Boundary Conditions for High Order Methods*

Report number: TRITA-NA-0325, ISRN KTH/NA/R--03/25--SE
Publication date: November 2003
E-mail of author: appelo@nada.kth.se

Department of Numerical Analysis and Computer Science
Royal Institute of Technology
SE-100 44 Stockholm
SWEDEN

**Abstract**

Using the framework introduced by Rowley and Colonius [14] we construct a discretely non-reflecting boundary condition for the one-way wave equation spatially discretized with an explicit fourth order centered difference scheme. The boundary condition, which can be extended to arbitrary order accuracy, is shown to be GKS-stable. We continue by deriving discretely non-reflecting boundary conditions for systems in two dimensions using the results for the scalar one dimensional case.

TRITA-NA-0325 • ISSN 0348-2952 • ISRN KTH/NA/R--03/25--SE

# 1 Introduction

When solving hyperbolic problems numerically on unbounded domains, the problem is confined to a smaller computational domain by introducing an artificial boundary. For many hyperbolic problems the correct boundary condition is that waves traveling across the boundary should not be reflected back. Boundary conditions which prevent waves from being reflected are often referred to as non-reflecting boundary conditions. Sometimes they may be referred to as transparent, artificial or absorbing boundary conditions.

Non-reflecting boundary conditions have been a matter of research for many decades. Some early explorers of the area were Lindeman [13] and Engquist and Majda [4], [5], who derived non-reflecting boundary conditions for the scalar wave equation. The works of Engquist and Majda have been an important source of inspiration in the construction of non-reflecting boundary conditions in different fields.

Boundary conditions of Engquist - Majda type are often formulated as a sequence of partial differential equations (PDE) which do not allow waves to travel back into the computational domain. The boundary conditions can be of different order, where a high order is equivalent with high order derivatives in the PDEs governing the boundary condition. When using such boundary conditions in numerical computations some possible drawbacks become apparent. The first is the question of how to discretize the high order (mixed) derivatives in a stable fashion. A way to handle this problem is to introduce auxiliary variables such that a system of first order PDEs is solved instead of the high order PDE on the boundary. However the issue of a stable discretization may still be present, especially when using numerical methods of high order. The second possible drawback relates to the fact that when any discretization procedure is used, spurious non-physical solutions are introduced. Boundary conditions which are non-reflecting for physical solutions may be highly reflective for its spurious counterpart. This indicates that it may be fruitful to consider *discretely* non-reflecting boundary conditions i.e. boundary conditions which are non-reflecting for both physical and spurious solutions.

The construction of a discretely non-reflecting boundary condition depends on the discretization procedure used, i.e. for each specific scheme a new boundary condition must be derived. In this paper we present the construction of a discretely non-reflecting boundary condition for the one-way wave equation where the standard five-point central difference approximation is used for the first order derivative in space.

In the recent paper [14] Rowley and Colonius have provided a framework for such construction. They construct boundary conditions for an implicit Padé three-point central difference scheme to illustrate their analysis. The discrete boundary conditions are then used to construct boundary conditions for the linearized Euler equations in two dimensions.

We consider a simpler model problem for the extension of our discrete scalar boundary condition to systems in two dimensions. The ideas presented here are directly applicable to any hyperbolic problem in two dimensions.

The Padé scheme, used in [14], is a fourth order implicit scheme. Widening the stencil from three to five points allows for an explicit fourth order scheme. However the issue of stability of the boundary condition becomes more involved.

The boundary conditions is extended to two space dimensions by combining exact continuous non-reflecting boundary conditions and the one dimensional discretely non-reflecting boundary condition. The resulting boundary condition is localized by the standard Padé approximation. By using auxiliary variables the two dimensional boundary condition can, in principal , be extended to high-order. However it is found by numerical experiments that the resulting method suffers from *boundary instabilities*.

Analysis of a related continuous problem suggests that the discrete boundary condition can be stabilized by adding tangential viscosity at the boundary. For the lowest order Padé approximation we are able to stabilize the discrete boundary condition. However, the results of the stabilized boundary condition is not satisfactory. The reflections are smaller than for the standard boundary condition but does not motivate the extra work needed to implement them.

# 2 Discretely Non-Reflecting Boundary Conditions in one Dimension

When solving hyperbolic problems with numerical methods, it is preferred to use explicit methods both in time and space. For truncated problems, the geometries of the outer boundary can often be chosen as preferred, e.g. as a box. For such simple geometry, the obvious choice of discretization is centered differences of high order in space combined with an explicit high order method (e.g. Runge-Kutta) in time. This combination yields an easy to implement, accurate and fast numerical method. By using centered differences in space and assuming that the grid is regular, at least close to the boundary, the errors produced by spurious waves may be controlled and minimized by discrete analysis.

In section 2.1 we recall some basic facts of finite difference schemes for hyperbolic problems. The notation of physical and spurious waves are introduced together with the discrete group and phase velocity.

In sections 2.2-2.3 we construct approximate discretely non-reflecting boundary conditions such that reflections caused by the coupling of spurious and physical modes are minimized.

## 2.1 Spurious and Physical Waves in One Dimensional Finite Difference Schemes

We begin by considering the scalar one-way wave equation

$$u_t + u_x = 0, \tag{1}$$

which admits solutions on the form

$$u(x,t) = e^{i(kx-\omega t)}. \tag{2}$$

Inserting (2) into (1), we obtain the **dispersion relation** $\omega \equiv \omega(k) = k$, where $k$ is the wave number and $\omega$ the frequency. For an equation with a dispersion relation, the **phase velocity**, $c_p$, and **group velocity**, $c_g$ can be defined as

$$c_p = \frac{\omega(k)}{k}, \quad c_g = \frac{d\omega(k)}{dk}.$$

For the equation (1), $c_p = c_g = 1$.

### Discrete Dispersion Relation

It is well known (see [16] for a detailed discussion) that a discretization of (1) will affect the dispersion relation and thereby the phase and group velocity. Different schemes have different dispersion relations and therefore they have to be analyzed separately.

In [14], Colonius and Rowley analyze a fourth order accurate, compact centered three point difference scheme. The advantage of using a compact three point scheme is that only one type of spurious waves will appear. The main disadvantage is that the scheme is implicit. Here, we will analyze the standard centered five point difference scheme of order four.

We start by introducing a regular grid in $x$, with mesh spacing $h$. Let $u_k$ denote the approximation of $u(x_k)$ where $x_k = kh$ and $k = 0, 1, \ldots, N$. We use the central finite difference approximation

$$\frac{\partial u(x_k)}{\partial x} \approx \frac{1}{12h}(-u_{k+2} + 8u_{k+1} - 8u_{k-1} + u_{k-2}). \tag{3}$$

of $u_x$ in(1) and obtain

$$(u_t)_k = \frac{1}{12h}(u_{k+2} - 8u_{k+1} + 8u_{k-1} - u_{k-2}). \tag{4}$$

The dispersion relation of (4) is

$$\omega(k) = \frac{4}{3h}\sin kh - \frac{1}{6h}\sin 2kh$$

In Figure 1 we compare dispersion relations and group velocities for the continuous problem and the discretized problem. Note that poorly resolved waves ($kh \approx \pi$) travel in the opposite direction, i.e. $c_g < 0$, to well resolved waves.

In Figure 1 (a) we can also see that for each frequency $\omega(k)$, there are two values of $k$ that satisfy the dispersion relation. The smaller one corresponds to a **physical** wave and the larger one corresponds to a **spurious** wave. For three point schemes, these two waves are the only type of waves that exist but for the fourth order scheme

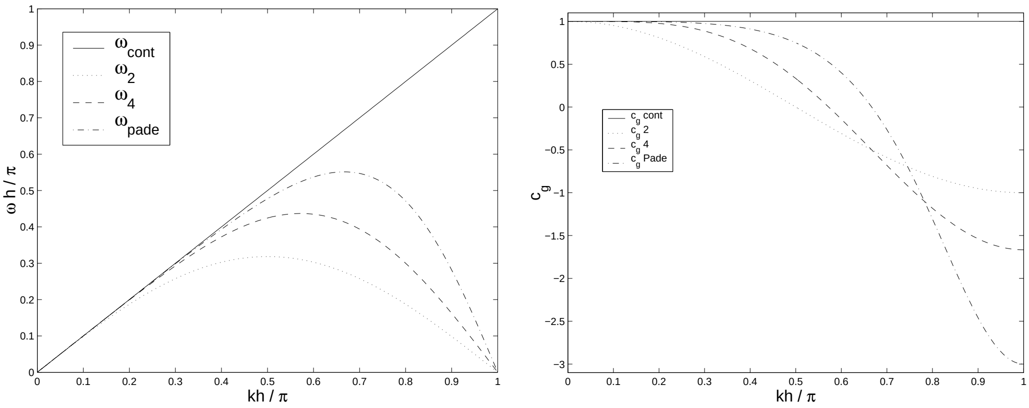


(a) Dispersion relations for different disc-tretizations.

(b) Group velocities for different disc-tretizations.

**Figure 1.** The notation $\omega_{cont}$, $\omega_2$, $\omega_4$and $\omega_{Pade}$ refers to the continuous, standard 2nd order centered scheme, standard 4th order scheme and the compact scheme [14].

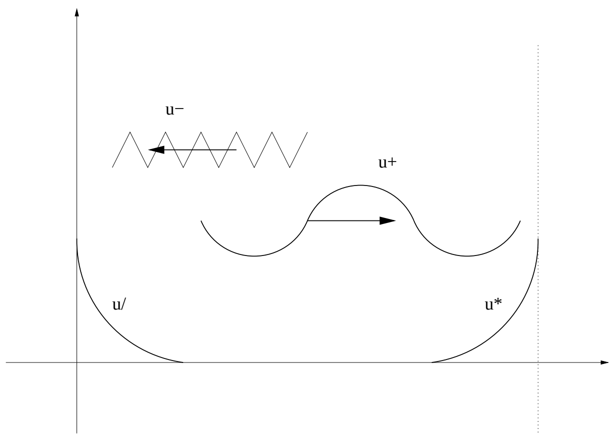


**Figure 2.** Different types of waves supported by standard five point centered difference scheme. $u^+$ corresponds to a physical right-going wave, $u^-$ to a spurious left-going wave, $u^*$ to a spurious wave decaying from the left and $u^{\div}$ to a spurious wave decaying from the right.

(3), there exist four values of $k$ that satisfies the dispersion relation, see section 2.2. Of these four, two correspond to wave solutions and two to damped wave solutions. This is illustrated in Figure 2.1. The two damped solutions are important for the stability but not for the non-reflectivity of the boundary condition. In short, stability of the boundary condition depends on weather they are uniquely determined.

## 2.2 Separation of Spurious and Physical Modes

By introducing a normal mode solution

$$u_k(t) = \hat{u} e^{i\omega t} \kappa^k,$$

with the property

$$u_{k+1} = \kappa u_k,$$

we obtain the characteristic equation of (4)

$$N(i\omega, \kappa) \equiv \left[\kappa^4 - 8\kappa^3 - i12\omega h\kappa^2 + 8\kappa - 1\right] = 0.$$

This equation has four nontrivial solutions

$$\begin{aligned} \kappa^+ &= 2 + \frac{1}{2}\xi - \frac{1}{2}\sqrt{\gamma + \theta}, \qquad & \kappa^- &= 2 - \tfrac{1}{2}\xi - \tfrac{1}{2}\sqrt{\gamma - \theta}, \\ \kappa^* &= 2 + \frac{1}{2}\xi + \frac{1}{2}\sqrt{\gamma + \theta}, \qquad & \kappa^\div &= 2 - \tfrac{1}{2}\xi + \tfrac{1}{2}\sqrt{\gamma - \theta}. \end{aligned}$$

Here

$$\begin{aligned} \eta &= (-18I\phi + 8I\phi^3 + \sqrt{-125 - 24\phi^2 + 48\phi^4})^{1/3}, \\ \xi &= \sqrt{16 + 8I\phi + (180 - 144\phi^2)/(18\eta) + 2\eta}, \\ \gamma &= 32 + 16I\phi - (180 - 144\phi^2)/(18\eta) - 2\eta, \\ \theta &= (448 + 384I\phi)/(4\xi), \\ \phi &= \omega h, \quad I = \sqrt{-1}. \end{aligned}$$

In order to distinguish the physical part of the solution from the spurious part we write the solution $u_k$ at a grid-point $k$ as

$$u_k = u_k^+ + u_k^- + u_k^* + u_k^\div,$$

where $u_k^@$ are normal modes that satisfy

$$N(i\omega, \kappa^@)u^@ = 0, \quad @ = \{+, -, *, \div\}.$$

The solutions $u^+$ and $u^-$ denote the physical and the spurious wave while $u^*$ and $u^\div$ are damped waves that decay from the right and left boundary respectively.

## 2.3 Approximate Non-Reflecting Boundary Conditions

We now seek approximate non-reflecting boundary conditions at the left ($k = 0$) and at the right ($k = N$) boundary. Following the ideas of Colonius [2] and Colonius and Rowley [14] we seek approximate boundary conditions of the form

$$\frac{du_0}{dt} = \frac{1}{c_1 h}\sum_{k=0}^{N_d} d_k u_k \equiv d_0^i u_0, \quad \frac{du_N}{dt} = \frac{1}{a_1 h}\sum_{k=0}^{N_d} b_k u_{N-k} \equiv d_N^o u_N, \tag{5}$$

where $a_1$, $b_k$, $c_1$, $d_k$, ($k = 0, \ldots, N_d$) are coefficients to be determined. Here $N_d$ is the order of the boundary condition. Consider first the left boundary.

Taking the Fourier transform in time and splitting $u$ into its different modes, (5) becomes

$$\begin{aligned} ic_1\omega h(u_0^+ + u_0^- + u_0^* + u_0^{\div}) &= \sum_{k=0}^{N_d} d_k(u_k^+ + u_k^- + u_k^* + u_k^{\div}) \\ \iff ic_1\omega h u_0^+ - \sum_{k=0}^{N_d} d_k(\kappa^+)^k u_0^+ &= \\ -ic_1\omega h(u_0^- + u_0^* + u_0^{\div}) + \sum_{k=0}^{N_d} d_k &\left[(\kappa^-)^k u_0^- + (\kappa^*)^k u_0^* + (\kappa^{\div})^k u_0^{\div}\right]. \end{aligned} \tag{6}$$

With $\phi = \omega h$, (6) becomes

$$d^+(\phi)u_0^+ = d^-(\phi)u_0^- + d^*(\phi)u_0^* + d^{\div}(\phi)u_0^{\div},$$

where

$$d^+(\phi) = c_1 i\phi - \sum_{k=0}^{N_d} d_k(\kappa^+)^k,$$

$$d^@(\phi) = -c_1 i\phi + \sum_{k=0}^{N_d} d_k(\kappa^@)^k, \quad @ = \{-, *, \div\}.$$

The exact non-reflecting boundary condition, $u_0^+ = 0$, would be satisfied if

$$d^@(\phi) = 0, \quad @ = \{-, *, \div\}.$$

It is not possible to fulfill $d^@(\phi) = 0$ for all $@ = \{-, *, \div\}$. However this is not necessary since $u^{\div}$ will be eliminated later and $u^*$ must be specified at the right boundary and will be very small at the left boundary. Thus only $d^-(\phi) = 0$ remains, this is equivalent with the condition obtained in [14].

Since $d^-(\phi)$ contains powers of $\kappa^-$ up to order $N_d$, it is natural to expand $\kappa^-(\phi)$ as a power series expansion around $\phi = 0$. The coefficients $c_1, d_0, \ldots$ are chosen such that $d^-(\phi)$ is minimized.

At the right boundary we use the same technique to find the boundary condition for $u_N$. Separating the spurious and physical modes of the ansatz (5) leads to the following expression

$$b^+(\phi)u_N^+ = b^-(\phi)u_N^- + b^*(\phi)u_N^* + b^{\div}(\phi)u_N^{\div},$$

where

$$b^+(\phi) = ac_1 i\phi - \sum_{k=0}^{N_d} \frac{b_k}{(\kappa^+)^k},$$
$$b^@(\phi) = -a_1 i\phi + \sum_{k=0}^{N_d} \frac{b_k}{(\kappa^@)^k}, \quad @ = \{-, *, \div\}.$$

The non-reflecting boundary condition for $u_N$ is $b^+(\phi) = 0$. For an equation with a left-going physical solution, e.g $v_t - v_x = 0$, the analysis is similar. The role of the spurious and physical solution at a boundary will be the opposite compared to an equation with a right-going physical solution. Using the notation introduced in (5), we may write boundary closures for the equation $v_t - v_x = 0$ as

$$\frac{dv_0}{dx} = d_0^o v_0, \quad \frac{dv_N}{dx} = d_N^i v_N.$$

### 2.4 Stability

When applying the scheme (3) to the gridpoint $k = 1$ we need information of both $u_0$ and $u_{-1}$. Above, $u_0$ has been determined to minimize the reflection at $k = 0$. The relation determining $u_{-1}$ must be chosen such that the boundary condition is stable. The mathematically correct boundary condition is $u(t, 0) = 0$, which together with (1) gives the relation $u(t, 0)_{xx} = 0$. First consider a three point wide stencil for the approximation of $(u_{xx})_{k=0}$, which yield the relation

$$u_{-1} = 2u_0 - u_1. \tag{7}$$

It can be shown that (7) yields a stable boundary condition for choices of $N_d$ at least up to $N_d = 8$. For example, consider $N_d = 1$ which gives the following relation for $u_0$

$$\frac{du_0}{dt} = -\frac{5}{3h}(u_0 + u_1). \tag{8}$$

To investigate the stability of the above boundary conditions for (4) we use Laplace transform technique (see e.g. [9]). We obtain the following eigenvalue problem

$$\tilde{s}\psi_j = \frac{1}{12h}(\psi_{j+2} - 8\psi_{j+1} + 8\psi_{j-1} - \psi_{j-2}), \quad \tilde{s} = sh. \tag{9}$$

There are two roots, $\kappa_\nu$, $\nu = 1, 2$, to the characteristic equation associated with (9), with $|\kappa_\nu| \leq 1$ for Re $\tilde{s} > 0$. The general solution of (9) with $\|\psi\|_h < \infty$ has the form

$$\psi_j = \sigma_1 \kappa_1^j + \sigma_2 \kappa_2^j, \quad \text{if } \kappa_1 \neq \kappa_2, \tag{10}$$

$$\psi_j = \sigma_1 \kappa_1^j + \sigma_2 j \kappa_1^{j-1}, \quad \text{if } \kappa_1 = \kappa_2. \tag{11}$$

First consider the case $\kappa_1 \neq \kappa_2$. Inserting the general solution (10) into the boundary conditions (7) and (8), we obtain the following equations for $\sigma_1$ and $\sigma_2$

$$\frac{\sigma_1}{\kappa_1} + \frac{\sigma_2}{\kappa_2} = 2\sigma_1 + 2\sigma_2 - \kappa_1\sigma_1 - \kappa_2\sigma_2,$$

$$\tilde{s}(\sigma_1 + \sigma_2) = \frac{5}{3}\left(-\sigma_1 - \sigma_2 - \kappa_1\sigma_1 - \kappa_2\sigma_2\right),$$

which may be formulated as a linear system of equations $C(\tilde{s}, \kappa_1, \kappa_2)\sigma = 0$. A necessary and sufficient condition for stability is that $\det C \neq 0$ for all Re $s \geq 0$. The determinant of $C$ is

$$\det C = \frac{(\kappa_1 - \kappa_2)(15\kappa_2\kappa_1 - 5\kappa_1 + 3\kappa_1\tilde{s}\kappa_2 - 5 - 3\tilde{s} - 5\kappa_2)}{3\kappa_2\kappa_1}$$

Clearly the first factor cannot be zero since $\kappa_1 \neq \kappa_2$. Assuming that the second factor is zero we solve for $\tilde{s}$

$$\tilde{s} = -\frac{5(1 + \kappa_1 + \kappa_2 - 3\kappa_1\kappa_2)}{3(1 - \kappa_2\kappa_1)}.$$

We want to show that there is no solutions Re $s \geq 0$. The the real part of the denominator is always positive except when $\kappa_1 = \kappa_2 = \pm 1$ which would be a contradiction to the assumption $\kappa_1 \neq \kappa_2$. By similar arguments arguments the real part of the numerator must always be positive. Hence, there are no solutions with Re $s \geq 0$ if $\kappa_1 \neq \kappa_2$.

Now consider the case $\kappa_1 = \kappa_2$. Inserting the general solution (11) into the boundary conditions (7) and (8) yields the determinant

$$\det C = \frac{-(3s\kappa_1^2 - 3s + 15\kappa_1^2 - 5 - 10\kappa_1)}{3\kappa_1^2} \equiv \frac{p_1(\kappa)}{3\kappa_1^2}.$$

The characteristic equation determining the root $\kappa_1$ is

$$p_2(\kappa) \equiv \kappa_1^4 - 8\kappa_1^3 - 12s\kappa_1^2 + 8\kappa_1 - 1.$$

If there is no solution to the system

$$\begin{aligned} p_1(\kappa) &= 0 \\ p_2(\kappa) &= 0 \end{aligned} \tag{12}$$

the boundary conditions are stable. The problem to determine if such solutions exist is known as the consistency problem and can be solved using Gröbner basis

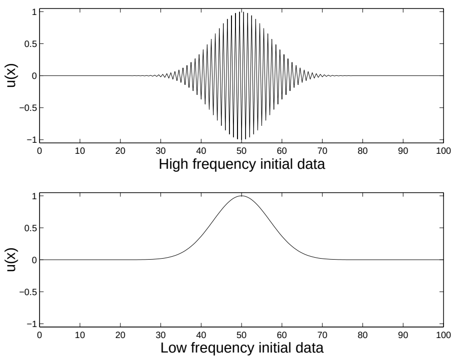


**Figure 3.** Initial data for experiments in one dimension.

[3]. Using the symbolic software Maple we are able to determine that there are no solutions to the system (12), hence the boundary conditions are stable.

Note that the boundary condition (7) is only second order which would degrade the overall accuracy of the method if used. Instead of (7) we use the fourth order accurate, five point, skew approximation of $u_{xx}$ which also will yield a stable boundary condition. Since this approximation is used, the overall order of the method will be four.

For the right boundary, a skew difference stencil $D_{-}^{q} u_{N-1}$ together with the non-reflective boundary conditions derived above can be shown to yield a stable boundary condition. If $q$ is chosen large enough the over all order of accuracy will be four.

## 2.5 Numerical experiments in 1D

To test the boundary condition, we consider the one-way wave equation (1) on the computational domain $x \in [0, 100]$, discretized with a regular grid. The spatial derivative is approximated by using the fourth order stencil (3) terminated using the discretely non-reflecting boundary conditions discussed in the previous section. The integration in time is performed with the standard fourth order Runge Kutta method. As a comparison, we use characteristic boundary conditions, i.e. $u(0,t) = 0$, together with extrapolation at the right boundary. The error is computed using a reference solution computed on a larger domain.

The boundary conditions are tested for two sets of initial data $u(x,0)$

$$
\begin{aligned}
u_{\text{high}}(x_k) &= (-1)^k u(x_k), \\
u_{\text{low}}(x_k) &= u(x_k), \\
u(x) &= e^{-\frac{(x-50)^2}{10^2}}.
\end{aligned}
$$

The initial data $u_{\text{high}}$ is oscillating with the highest frequency allowed on the grid while the initial data $u_{\text{low}}$ is smooth, see Figure 3. In Figure 4 the error for different

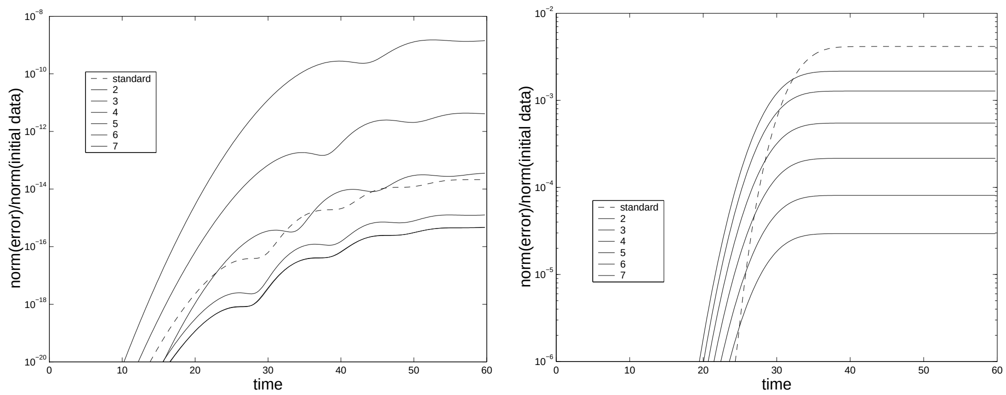


(a) The $l_2$ error on the computational domain for the smooth initial data for different $N_d$ compared with characteristic boundary conditions. For $N_d > 4$ the discretely non-reflecting boundary condition outperforms the characteristic boundary condition.

(b) The $l_2$ error on the computational domain for the non-smooth initial data for different $N_d$ compared with characteristic boundary conditions. Here the discretely non-reflecting boundary condition is more efficient then characteristic boundary conditions for all $N_d$.

**Figure 4.**

$N_d$ is compared to the error introduced by characteristic boundary conditions. It is clear that for large $N_d$, the discretely non-reflecting boundary conditions are more efficient than characteristic boundary conditions independent of the smoothness of the initial data. Especially for the non-smooth initial data, the discretely non-reflecting boundary condition works well.

# 3 Continuous Non-Reflecting Boundary Conditions

An important feature of linear systems of hyperbolic equations is that it is possible to separate in-going and out-going parts of the solution at a boundary. The decomposition of the solution at a boundary is obtained by using the theory of characteristics. This decomposition of the solution is closely related to the well-posedness of the problem. The necessary condition for well-posedness is that in-going components of the solution must be specified by the boundary conditions at each boundary.

If the boundary condition is to be well-posed and non-reflecting, the in-going modes should be put to zero. This will prevent reflection of the solution back into the domain. Below, we construct well-posed, non-reflecting boundary conditions for a simple model problem in two dimensions. For a complete discussion of construction of continuous non-reflecting boundary conditions for linear hyperbolic systems see [14] or [6].

### 3.1 A Model Problem in 2D

Consider the system

$$w_t + Aw_x + Bw_y = 0, \tag{13}$$

on the domain $0 \leq x \leq L$, $-\infty < y < \infty$, $t > 0$, where

$$w = \begin{bmatrix} u \\ v \end{bmatrix}, \quad A = \begin{bmatrix} 1 & 0 \\ 0 & -1 \end{bmatrix}, \quad B = \begin{bmatrix} 0 & 1 \\ 1 & 0 \end{bmatrix}.$$

To derive non-reflecting boundary conditions for (13) at $x = 0$ and $x = L$, we take the Laplace transform in time and the Fourier transform in the y direction. The transformed system is

$$\hat{w}_x = -A^{-1}(sI + ikB)\hat{w},$$

where $(s, k)$ are the duals of $(t, y)$. Let $z = ik/s$, then we may write

$$\hat{w}_x = -sA^{-1}(I + zB)\hat{w} \equiv -sM(z)\hat{w}. \tag{14}$$

Since (13) is a hyperbolic problem, we can decompose the solution into left and right-going waves. The right-going waves are those corresponding to positive eigenvalues of $M(z)$ at $z = 0$ and the left-going those that correspond to negative eigenvalues.

The eigenvalues and left eigenvectors of $M(z)$ are (here the subscript R denotes right-going and L denotes left-going waves)

$$\lambda_R = \sqrt{1 - z^2}, \quad Q_R = \begin{bmatrix} 1 + \sqrt{1 - z^2} \\ z \end{bmatrix}^T,$$

$$\lambda_L = -\sqrt{1 - z^2}, \quad Q_L = \begin{bmatrix} 1 - \sqrt{1 - z^2} \\ z \end{bmatrix}^T.$$

Using the diagonalization

$$QMQ^{-1} = \begin{bmatrix} \lambda_R & 0 \\ 0 & \lambda_L \end{bmatrix},$$

where

$$Q = \begin{bmatrix} Q_R \\ Q_L \end{bmatrix},$$

to decouple the system (14) into two scalar equations, it is easy to see that the exact non-reflecting boundary conditions for (13) are

$$\begin{aligned} Q_R\,\hat{w} &= 0 \text{ at } x = 0, \\ Q_L\,\hat{w} &= 0 \text{ at } x = L. \end{aligned} \tag{15}$$

The exact non-reflecting boundary condition (15) contains the non-rational function $\sqrt{1 - z^2}$, which does not have an explicit inverse transform. Consequently, the corresponding boundary condition in the physical space will be exact but nonlocal in time and space. This non locality is undesirable and leads to expensive and cumbersome implementation of the boundary conditions when used for computations. To localize these boundary conditions, $\sqrt{1-z^2}$ may e.g. be replaced by some rational approximant, which can be transformed back directly.

### 3.2 Rational Approximants and Non-Reflecting Boundary Conditions

The problem of approximating the function $\sqrt{1-z^2}$ in the context of non-reflecting boundary conditions has been extensively studied in the literature. See e.g. Engquist and Majda [4]. Trefethen and Halpern [15] provides detailed studies of different type of approximations (Padé, Chebyshev and least-squares).

In this paper we consider only the Padé approximations which yield well-posed, see [15], boundary conditions in exactly the diagonals, $m = n$ and $m = n+2$ of the table of approximants $(m, n)$.

By replacing $\sqrt{1-z^2}$ with the Padé approximant, in $Q_R$ and $Q_L$, we obtain the following approximate non-reflecting boundary conditions

$$\begin{aligned} E_R\,\hat{w} &= 0 \text{ at } x = 0, \\ E_L\,\hat{w} &= 0 \text{ at } x = L. \end{aligned} \tag{16}$$

## 4 Discretely Non-Reflecting Boundary Conditions in 2D

To derive a discretely non-reflecting boundary condition in two dimensions, we can use the exact boundary conditions, discussed in section 3.1, together with the discretely non-reflecting boundary conditions discussed in section 2.3. Since the discretely non-reflecting boundary conditions are directly applicable for one-way equations we use the exact continuous boundary conditions for (13) to obtain one-way equations.

Consider again the transformed version of the system (13)

$$\hat{w}_x = -sM(z)\hat{w}, \tag{17}$$

with the exact non-reflecting boundary conditions (15)

$$\begin{aligned} Q_R\,\hat{w} &= 0 \text{ at } x = 0, \\ Q_L\,\hat{w} &= 0 \text{ at } x = L. \end{aligned}$$

Now define the matrix

$$Q(z) = \begin{bmatrix} Q_R \\ Q_L \end{bmatrix},$$

and let $T(z)$ be the matrix composed by the right eigenvectors to $M(z)$ such that

$$T^{-1}MT = \begin{bmatrix} \lambda_R & 0 \\ 0 & \lambda_L \end{bmatrix} \equiv \Lambda. \tag{18}$$

The matrix $C = QT$ is diagonal and invertible since the boundary conditions are well posed. Hence, $Q$ is also invertible and we may use the transformation $g = Q\hat{w}$ in (17) with the result

$$\frac{d}{dx}Q\hat{w} = -s(QMe^{-1})Q\hat{w} \Rightarrow$$
$$\frac{d}{dx}g = -s\Lambda g.$$

We obtain two decoupled one way equations

$$\frac{d}{dx}g^R = -s\lambda_R\, g^R, \quad \frac{d}{dx}g^L = -s\lambda_L\, g^L.$$

Introduce a regular grid in $x$, with mesh spacing $h$, and let $g_k$ denote the approximation of $g(x_k)$ at $x_k = kh$, $k = 0, 1, \ldots, N$. The discrete non-reflecting boundary conditions at the left and right boundary, respectively, are

$$\begin{aligned} d_0^i\, g_0^R &= -s\lambda_R\, g_0^R, \quad d_0^o\, g_0^L = -s\lambda_L\, g_0^L, \\ d_N^i\, g_N^R &= -s\lambda_R\, g_N^R, \quad d_N^o\, g_N^L = -s\lambda_L\, g_N^L. \end{aligned}$$

Defining

$$D_L = \begin{bmatrix} d_0^i & 0 \\ 0 & d_0^o \end{bmatrix}, \quad D_R = \begin{bmatrix} d_N^o & 0 \\ 0 & d_N^i \end{bmatrix},$$

and transforming back to $\hat{w}$, we obtain the boundary conditions

$$\begin{aligned} -sQ(z)M(z)\hat{w}_0 &= D_L Q(z)\hat{w}_0, \\ -sQ(z)M(z)\hat{w}_N &= D_R Q(z)\hat{w}_N. \end{aligned} \tag{19}$$

The boundary conditions (19) need to be transformed back to the physical space to be useful. Since $Q(z)$ contains non-rational functions of $z$, this will lead to boundary conditions which are nonlocal both in time and space. By replacing $Q(z)$ by a rational approximant $E(z)$, as described in section 3.2, the boundary conditions (19) become

$$\begin{aligned} E(z)\frac{\hat{w}_0}{dx} &= D_L E(z)\hat{w}_0, \\ E(z)\frac{\hat{w}_N}{dx} &= D_R E(z)\hat{w}_N. \end{aligned} \tag{20}$$

Here we have used the interior equations (17). Since $E(z)$ is a rational function (20) can be transformed to a local boundary condition by inverse Laplace and Fourier transform.

Using a high order approximant in the construction of $E(z)$ will result in a boundary condition containing high order mixed derivatives in t and y. In general high order derivatives are undesirable since they are difficult to discretize in a stable and accurate manner. Especially, this is true when using a high order scheme in the interior.

To obtain boundary conditions containing no mixed derivatives, auxiliary variables may be introduced. These variables can be chosen in many ways. Here we chose the approach suggested in Rowley and Colonius [14]. Alternative approaches can be found in e.g. Hagstrom and Harihan [8] or Givoli and Neta [7].

### 4.1 Non-Reflecting Boundary Conditions using Auxiliary Variables

We start by multiplying each row of equation (20) by its least common denominator to obtain the following system

$$E'(z)\frac{\hat{w}_0}{dx} = D_L E'(z)\hat{w}_0, \tag{21}$$

$$E'(z)\frac{\hat{w}_N}{dx} = D_R E'(z)\hat{w}_N, \tag{22}$$

where

$$E'(z) = E_0 + zE_1 + \cdots + z^p E_p.$$

Introduce auxiliary variables $h_j$ such that (21) becomes

$$\begin{aligned} E_0\frac{\partial w_0}{\partial x} &= D_L E_0 w_0 + \frac{\partial}{\partial y}(F_0 w_0 + h_1), \\ \frac{\partial h_j}{\partial t} &= D_L E_j w_0 + \frac{\partial}{\partial y}(F_j w_0 + h_{j+1}), \quad j = 1, \dots, p-1 \\ \frac{\partial h_p}{\partial t} &= D_L E_p w_0 + \frac{\partial}{\partial y}(F_p w_0), \end{aligned} \tag{23}$$

where

$$\begin{aligned} F_0 &= E_1 A^{-1}, \\ F_j &= E_j A^{-1} B + E_{j+1} A^{-1}, \quad j = 1, \dots, p-1 \\ F_p &= E_p A^{-1} B. \end{aligned}$$

The boundary condition (23) is easy to implement and the extra amount of memory needed for the auxiliary variables is proportional to the order of the rational approximant. For the boundary conditions at the right boundary, simply replace $w_0$ by $w_N$.

### 4.2 Stability of the Non-Reflecting Boundary Conditions

Consider (23) with the Pade expansion (0,0) and $N_d = 2$ for the operators $d_0^i$ and $d_0^o$. For these choices, (23) become

$$\begin{aligned}\frac{\partial u_0}{\partial x} &= d_0^i u_0 + \frac{1}{2}\frac{\partial}{\partial y}(-v_0 + h_1),\\ \frac{\partial v_0}{\partial x} &= d_0^o v_0\\ \frac{\partial h_1}{\partial t} &= d_0^i v_0\end{aligned} \tag{24}$$

with

$$d_0^i q_0 = \frac{3}{5h}(q_0 + q_1), \quad d_0^o q_0 = \frac{1}{h}(-q_0 + q_1).$$

In the gridpoints next to the boundary a skew approximations for the x-derivatives of $u$ and $v$ are used. When approximating $u_x$, $\tilde{d}^i$ is used and when approximating $v_x$, $\tilde{d}^o$ is used. The skew operators are chosen as

$$\tilde{d}^i q_1 = \frac{1}{12h}(-6q_0 - q_1 + 8q_2 - q_3), \quad \tilde{d}^o q_1 = \frac{1}{h}(q_2 - q_1). \tag{25}$$

When we solve (13) numerically, using these boundary conditions at $x = 0$ and periodic boundary conditions in $y$ we experience instability. The instability appear at $x = 0$. The unstable solution is highly oscillatory in y and decay rapidly into the computational domain. The decay and the oscillations indicated that the instabilities are so called *boundary instabilities* [12]. To further investigate this problem, we analyze a continuous model problem.

### 4.3 Stability of a Model Problem

By investigating the well-posedness of a continuous model problem, similar in structure to (24), we hope to identify the mechanisms responsible for the instability of the non-reflecting boundary conditions (24). The problem we consider is equation (13) with initial data $w(0, x, y) = f(x, y)$ on the domain $\{0 \le x < \infty, -\infty < y < \infty, t > 0\}$ closed with the boundary condition

$$u_x = -(u + 2u_t + u_y - \varepsilon u_{yy}), \quad \varepsilon \ge 0. \tag{26}$$

We will use the Laplace transform technique [11] to determine the well-posedness of the stated problem. The problem (13), (26) is said to be ill-posed in any sense if there exist a solution

$$w = e^{st+iky}\Psi(x), \quad \text{Re } s > 0, \ \|\Psi(x)\| < \infty, \ k \text{ real}.$$

For the problem (13), (26) we have the following lemma.

**Lemma 1** *The problem (13), (26) is ill-posed for* $\varepsilon = 0$ *and well-posed for* $\varepsilon > \frac{4+\sqrt{106}}{45}$.

**Proof of Lemma 1** Inserting the ansatz $w = e^{st+iky}\Psi(x)$ into (13) yields the eigenvalue problem

$$(sI + ikB)\Psi + A\Psi_x = 0, \tag{27}$$

with the eigenvalues $\lambda_1 = -\lambda_2 = -\sqrt{s^2+k^2}$. The solution of (27) satisfying $\|\Psi(x)\| < \infty$ is

$$\Psi(x) = \sigma e^{-\sqrt{s^2+k^2}x}\Phi. \tag{28}$$

Here $\Phi = [\phi_1, \phi_2]^T = \left[-s\sqrt{s^2+k^2}, ik\right]^T$ is the eigenvector corresponding to $\lambda_1$. To be a solution, (28) must fulfill the boundary condition (26). This leads to the algebraic relation

$$-\sqrt{s^2+k^2} = -(1 + 2s + ik + \varepsilon k^2), \tag{29}$$

which must hold for $\sigma \neq 0$. By solving explicitly for s

$$s = -\frac{2(1+\varepsilon k^2)}{3} - \frac{i2k}{3} + \frac{1}{3}\sqrt{1 + 2\varepsilon k^2 + i2k + \varepsilon^2 k^4 + i2k^3\varepsilon + 2k^2}.$$

For $\varepsilon = 0$ we have

$$s = -\frac{2}{3} - \frac{i2k}{3} + \frac{1}{3}\sqrt{1 + i2k + 2k^2}.$$

For $k = 0$ we have Re $s = -2/3$ so the problem is well posed for data which does not vary in the y- direction. However, for large $k$, Re $s \sim k$ and we conclude that there exist some $k_0$ such that the problem is ill-posed for all $k > k_0$. For $\varepsilon > 0$ a sufficient condition for well-posedness is that

$$\begin{aligned} 2(1+\varepsilon k^2) > |\sqrt{1 + 2\varepsilon k^2 + i2k + \varepsilon^2 k^4 + i2k^3\varepsilon + 2k^2}| = \\ ((1 + 2k^2(1+\varepsilon) + \varepsilon^2 k^4)^2 + (2k + 2k^3\varepsilon)^2)^{1/4} \end{aligned}$$

Taking both sides raised to the fourth power gives

$$\begin{aligned} 16 + 64\varepsilon k^2 + 96\varepsilon^2 k^4 + 64\varepsilon^3 k^6 + 16\varepsilon^4 k^8 > \\ 1 + (8+4\varepsilon)k^2 + (2\varepsilon^2 + (2+2\varepsilon)^2 + 8\varepsilon)k^4 + (2(2+2\varepsilon)\varepsilon^2 + 4\varepsilon^2)k^6 + \varepsilon^4 k^8. \end{aligned} \tag{30}$$

By inspection of the coefficients it is clear that (30) hold if $\varepsilon > \frac{4+\sqrt{106}}{45}$. □

For the case $\varepsilon = 0$, the solution will be $\hat{w} = e^{st+iky-\sqrt{s^2+k^2}x}\Phi$. This solution grows exponentially in time, oscillates rapidly in the y direction (k is large) but decays exponentially in the x direction. Usually, this kind of instability is referred to as a *boundary instability*. When this type of instability occurs in an numerical method, the remedy is to add a small number of tangential viscosity to stabilize the numerical method. The addition of tangential viscosity can be understood by the above analysis. Since the boundary condition (26) has a structure similar to the discrete boundary condition (23), it is reasonable to expect that instabilities observed in the numerical computations may be removed by adding a sufficient amount of tangential viscosity.

### 4.4 Stabilized Non-Reflecting Boundary Condition

We want to add viscosity to stabilize the boundary conditions (24). Viscosity is introduced by adding the term $\varepsilon v_{yy}$ to the first row of the equations (13). This is equivalent to modify the the matrix $M(z)$ to

$$\tilde{M}(z) = \begin{bmatrix} 1+\varepsilon k^2 & z \\ -z & -1 \end{bmatrix}.$$

This modification is used at the two gridpoints next to the boundary.

To analyze the stabilized boundary conditions, we use the Laplace transform technique on the halfplane problem, defined by the equations (13), (24) on $\{0 \leq x < \infty, -\infty < y < \infty, t > 0\}$. Taking the Fourier transform in y direction and the Laplace transform in time yield the following relations at the gridpoints $x_i$, $i = \{0, 1, 2\}$

$$\begin{aligned} -sE'(z)M(z)\hat{w}_0 &= D_L E'(z)\hat{w}_0, \\ -s\tilde{M}(z)\hat{w}_1 &= \tilde{D}\hat{w}_1, \\ -s\tilde{M}(z)\hat{w}_2 &= D^{(4)}\hat{w}_2. \end{aligned} \tag{31}$$

The first relation contains the non-reflecting boundary condition (24). The second equation contains the operator $\tilde{D} = \text{diag}(\tilde{d}^i, \tilde{d}^o)$ defined in (25). The operator $D^{(4)}$ is the usual fourth order accurate approximation of the derivative and the matrix $\tilde{M}(z)$ is modified as described above.

Away from the boundary, the solution is determined by the equation

$$-sM(z)\hat{w}_k = D^{(4)}\hat{w}_k, \quad k > 2. \tag{32}$$

The general solution of (32), satisfying $\|\hat{w}_k\|_h < \infty, \forall k$ with Re $s > 0$, is

$$\hat{w}_k = \left[\sigma_R^{+}(\kappa_R^{+})^k + \sigma_R^{\div}(\kappa_R^{\div})^k\right]\Psi_R(z) + \left[\sigma_L^{-}(\kappa_L^{+})^k + \sigma_L^{*}(\kappa_L^{*})^k\right]\Psi_L(z). \tag{33}$$

Here the $\sigma_R^{+}, \sigma_R^{\div}, \sigma_L^{-}, \sigma_L^{*}$ are constants to be determined by the relations (31). The subscript $L$ correspond to a left-going mode and $R$ to a right-going. The vectors

$\Psi_L(z)$ and $\Psi_R(z)$ are the right eigenvectors of the matrix $M(z)$ corresponding to the eigenvalues $\lambda_L$ and $\lambda_R$. The different $\kappa$ are the roots to the equations

$$\kappa_R^4 - 8\kappa_R^3 + 12hs\sqrt{1-z^2}\kappa_R^2 + 8\kappa_R - 1 = 0,$$
$$\kappa_L^4 - 8\kappa_L^3 - 12hs\sqrt{1-z^2}\kappa_L^2 + 8\kappa_L - 1 = 0,$$

satisfying $|\kappa| < 1$. It is possible to show, see [9], that for Re $s > 0$ there exist exactly two solutions with amplitude less than one to each of the above characteristic equations.

Inserting the solution (33) into the boundary conditions at $x_1$ and $x_2$ together with the boundary conditions at $x_0$, where $\hat{u}_0$ and $\hat{v}_0$ are considered as unknowns, yields a system of equations

$$C(\tilde{s}, k) \begin{bmatrix} \hat{u}_0 \\ \hat{v}_0 \\ \sigma_R^+ \\ \sigma_R^{\div} \\ \sigma_L^- \\ \sigma_L^* \end{bmatrix} = 0.$$

Here $\tilde{s} = sh$ and $C(\tilde{s}, k)$ is a 6 by 6 complex matrix with elements that are nonlinear in $\tilde{s}$ and $k$.

The numerical method defined by (31) and (32) is unstable if the determinant of $C(\tilde{s}, k)$ vanish for any $(\tilde{s}, k)$ with Re $\tilde{s} > 0$. Due to the nonlinear structure of the elements, we have been unable to find analytic expressions for the zeros of $\det C(\tilde{s}, k)$. However, by numerical examination of $\det C(\tilde{s}, k)$, we are able to determine if there are any zeros in the right half of the complex $\tilde{s}$ plane.

First, considering the case $\varepsilon = 0$ we find a zero which moves as the parameter $k$ changes. For small $k$ it will move towards the left halfplane, and for large $k$ into the right, i.e. the method is stable for small $k$ but not for large $k$. This behavior is similar to that of the model problem. As for the model problem, we add tangential viscosity at the boundary to remove the instability.

In Figure 5 we have plotted the location of the zeros of $\det C(\tilde{s}, k)$ in the $\tilde{s}$ plane as a function of k for different amounts of viscosity. By increasing $\varepsilon$ we see that the curves move towards the stable left halfplane. Empirical studies show that the amount of viscosity needed, for all zeros in the right halfplane to disappear, is proportional to the stepsize $h$ with some modest constant.

For boundary conditions using higher order Padé approximations, we have also experienced instabilities which seem to be related to large wavenumber $k$. However, we have not been able to remove these instabilities by adding viscosity.

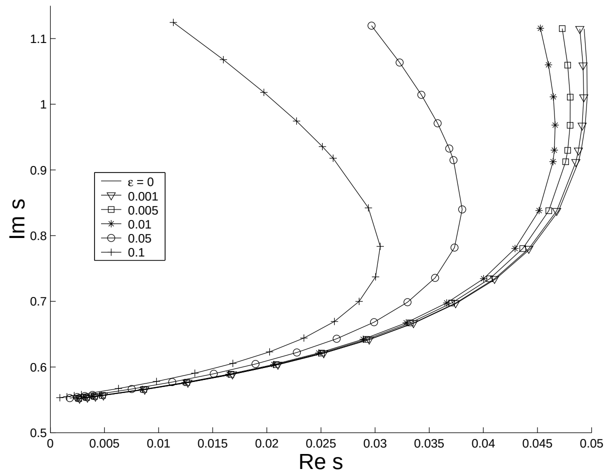


**Figure 5.** The location of the zeros of $\det C(\tilde{s}, k)$ in the $\tilde{s}$ plane as a function of $k$ for different amount of viscosity. The zeros start in the lower left part of the Figure and move along the lines to the right as $k$ increases.

### 4.5 Numerical Experiments in 2D

Consider the problem (13) with the initial data

$$w(x, y, 0) = \begin{pmatrix} 1 \\ -1 \end{pmatrix} e^{-\frac{(x-0.5)^2+(y-0.5)^2}{0.1^2}},$$

on the domain $(x, y) \in [0, 4] \times [0, 1]$ with periodic boundary conditions in the y direction and the boundary condition (23) on the left boundary. We only want to consider effects from the left boundary so we choose the placement of the right boundary such that it does not influence the measured error from the left boundary. The error measured is the $L_2$ error in the domain $(x, y) \in [0, 0.1] \times [0, 1]$ and is calculated from a reference solution obtained on a larger domain. The results are compared with results obtained when using characteristic boundary conditions, see Figure 6. The boundary condition is better than the characteristic boundary condition for all times. However the increase in performance is small compared with the additional work needed to implement (23).

## 5 Summary

Discretely non-reflecting and stable boundary conditions for hyperbolic systems in one space dimension have been derived. The boundary conditions work well for both spurious and physical waves. The performance increases with the order $N_d$.

The boundary conditions is extended to two space dimensions by combining exact continuous non-reflecting boundary conditions and the one dimensional discretely non-reflecting boundary condition. The resulting boundary condition is localized by

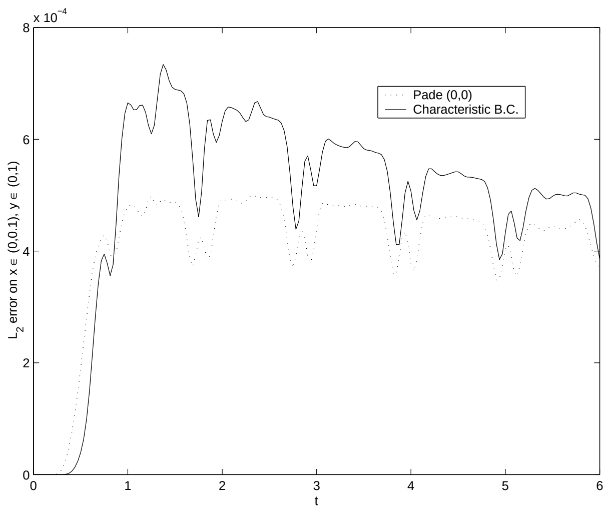


**Figure 6.**

the standard Padé approximation. By using auxiliary variables the two dimensional boundary condition can, in principal , be extended to high-order. However it is found by numerical experiments that the resulting method suffers from *boundary instabilities.* Analysis of a related continuous problem suggests that the discrete boundary condition can be stabilized by adding tangential viscosity at the boundary. For the lowest order Padé approximation we are able to stabilize the discrete boundary condition. However, the results of the stabilized boundary condition is not satisfactory. The reflections are smaller than for the characteristic boundary condition but does not motivate the extra work needed to implement them.

# References

[1] F. Collino and P.B. Monk, *Optimizing the perfectly matched layer*, Comput. Methods Appl. Energ., pp. 157–171, **164**, (1998).

[2] T. Colonius, *Numerically nonreflecting boundary and interface conditions for compressible flow and aeroacoustic computations*, AIAA Journal, pp. 1126 **35** (1997).

[3] D. Cox, J. Little and D. O'Shea, *Ideals, Varieties and Algorithms*, Undergraduate Texts in Mathematics. (Springer-Verlag, New York 1992)

[4] B. Engquist and A. Majda, *Absorbing boundary conditions for the numerical simulation of waves*, Math. Comp., pp. 629, **31**, (1977).

[5] B. Engquist and A. Majda, *Radiation Boundary Conditions for Acoustic and Elastic wave Calculations*, Comm. Pure. Appl. Math., pp. 313-357, **32**, (1979).

[6] M. Giles, *Nonreflecting Boundary Conditions for Euler Equation Calculations*, AIAA Journal, 28:2050-2058, (1990).

[7] D. Givoli and B. Neta, *High-order non-reflecting boundary scheme for time dependent waves*, J. Comput. Phys., 186 :24-46, (2003).

[8] J. W. Goodrich and T. Hagstrom, *Accurate Algorithms and Radiation Boundary Conditions for Linearized Euler Equations*, AIAA Paper 96-1600, 1996.

[9] B. Gustafsson, H-O. Kreiss and J. Oliger, *Time Dependent Problems and Difference Methods*, Pure and Applied Mathematics. (Wiely, New York 1995)

[10] T. Hagstrom and S.I. Harihan, *A formulation of asymptotic and exact boundary conditions using local operators*, Appl. Numer. Math., pp. 403-416, **27**, (1998).

[11] H-O. Kreiss and J. Lorenz, *Initial-Boundary Value Problems and the Navier-Stokes Equations*, Pure and Applied Mathematics. (Academic Press, 1989)

[12] H-O. Kreiss, N. A. Petersson amd J. Ystrom, *Difference approximations for the second order wave equation*, SIAM J. Numer. Anal., 40:1940-1967, (2002).

[13] E. L. Lindman, *"Free space" Boundary Conditions for the Time Dependent Wave Equation* , J. Comput. Phys., pp. 66-78, **18** (1975).

[14] C. W. Rowley and T. Colonius, *Discretely Nonreflectiing Boundary Conditions for Linear Hyperbolic Systems*, J. Comput. Phys., pp. 500-538, **157** (2000).

[15] L.N. Trefethen and L. Halpern, *Well-Posedness of One-Way Wave Equations and Absorbing Boundary Conditions*, Math. Comp., pp. 421–435, **176**, (1986).

[16] L.N. Trefethen, *Group Velocity in Finite Difference Schemes*, SIAM review, pp. 113–136, **24**, (1982).